IEEE Access
Multidisciplinary | Rapid Review | Open Access Journal

SPECIAL SECTION ON UNDERWATER WIRELESS COMMUNICATIONS AND NETWORKING

Received December 15, 2017, accepted March 4, 2018, date of publication March 22, 2018, date of current version May 9, 2018.

Digital Object Identifier 10.1109/ACCESS.2018.2815743

Performance Evaluation of LOS and NLOS Vertical Inhomogeneous Links in Underwater Visible Light Communications

NOHA ANOUS[1], MOHAMED ABDALLAH[2], (Senior Member, IEEE), MURAT UYSAL[3], (Senior Member, IEEE), AND KHALID QARAQE[1], (Senior Member, IEEE)

[1]Electrical and Computer Engineering, Texas A&M University at Qatar, Doha 23874, Qatar
[2]College of Science and Engineering, Hamad Bin Khalifa University, Qatar Foundation, Doha 34110, Qatar
[3]Department of Electrical and Electronics Engineering, Özyeğin University, 34794 Istanbul, Turkey

Corresponding author: Noha Anous (noha.anous@qatar.tamu.edu)

This work was made possible by the NPRP award [NPRP 8-648-2-273] from the Qatar National Research Fund (a member of the Qatar Foundation). The statements made herein are solely the responsibility of the author[s].

ABSTRACT In this paper, underwater visible light communication (UWVLC) vertical links are modeled and evaluated, taking account of the inhomogeneous nature of underwater (UW) environment. An equivalent simplified model of stratified N layers is employed in which variations in refractive index and attenuation profiles across UW depth are considered. A generalized path loss expression is deduced which allows estimation of the vertical link loss prior to link design. Mathematical expressions of the received power for line-of-sight (LOS) and non-line-of-sight (NLOS) links between transmitters (Tx) and receivers are deduced. We evaluate the performance by computing the received power and bit error rate for inhomogeneous underwater links. Numerical examples are used to illustrate the proposed models. Deviations from expected results when considering a homogeneous underwater model are discussed. A simple underwater bilayer model is then introduced, which is considered a rough approximate model in comparison to the stratified N layers model. This model assists in estimating the UW link behavior without extensive calculations. The conditions necessary for applying this model are discussed and justified. Moreover, the effects of Tx orientation along with narrowing the transmitted light cone on LOS and NLOS vertical links are examined. A Tx power saving of 30%–50% in UWVLC links is proved to be achieved by rotating the Tx and narrowing its emitted light cone.

INDEX TERMS BER, energy efficient, inhomogeneous, light focusing, link budget, power saving, stratified layers, Tx orientation, underwater (UW), VLC.

I. INTRODUCTION

Underwater communications has started as a military field of interest in World War II. However, recently it has drawn the attention to a large number of potential civilian applications such as environmental monitoring, underwater archeology, and disaster precaution and analysis. In some of these applications, UW requires establishing a vertical communication link between these underwater objects and sea-level or off-shore transceivers. For example, a human explorer at a depth of 35,756 ft. ∼10,898 m below sea-level (recorded as the deepest possible point reached by a human in early 2012) needs a connection with an off-shore transceiver for safety. Also, in the case of airplane disasters, the black boxes can send beacon signals from a maximum of 6000 m depth for about 30 days [1]–[4].

The unguided transmission in underwater environment has been realized by radio frequency (RF), acoustic as well as VLC links. RF propagation underwater suffers from relatively high attenuation which limits its usage to short communication links. Acoustics and VLC can be viewed as complementary technologies in achieving the required performance of underwater systems. One example is having a control platform which broadcasts to underwater sensor nodes (SNs) using acoustic communication whereas the SNs communicate with each other through VLC. However, acoustic links suffer from low data rates (several kilobits

per second), high communication latency (order of seconds), with harmful effects to marine life. Moreover, acoustic transceivers are bulky, costly with high power consumption. These disadvantages serve as an incentive for seeking all-UWVLC links as a viable alternative technology to RF, acoustic or acoustic-VLC hybrid systems [2]–[4].

UWVLC links may be divided into two major types; horizontal and vertical/slant links. Horizontal links have been extensively studied focusing on increasing data rates, propagation lengths and reducing the UW turbulence effect [5]–[9]. Surveys over channel models are available in literature [2]–[4]. One scenario of slant links arousing from non-line-of-sight (NLOS) configurations is discussed in [10]. Vertical links formed due to shore to undersea communications are studied in [11]–[12] with considerations of waves height, wind speed and sea surface slopes. However, an important parameter such as water density variations with the vertical depth have been overlooked in the above presented models. In [13]–[15] the variation in UW environment with depth is considered, but applied only to study the light beam displacement due to refractive index variations as discussed hereafter. For the best of our knowledge, vertical link models and their performance have not been previously studied.

The optical properties of underwater environment is dependent upon several parameters including salinity (S), temperature (T) and pressure (P) [16]. In the literature, underwater media is mostly treated as a homogeneous medium with single S, T and P values. This might be an acceptable approximation for horizontal links in still water. However, in vertical links, pressure increases by $10dbar$ every $10m$ of depth in addition to a significant decrease in water temperature from 25° to may be near 0° Celsius [17]. These variations among variations in salinity, directly affect the refractive index profile of water causing it to be more of a gradient profile versus depth rather than a single valued constant. On the other hand, variations in chlorophyll concentrations -among other organic and inorganic UW substances- with underwater depth result in an attenuation coefficient profile versus depth [4], [13]. These depth dependent profiles suggest the necessity of considering the effect of such inhomogeneous models of underwater environment on LOS and NLOS optical links. In addition to examining the possible performance deviations resulting from links employing homogeneous models.

In this work, a mathematical model of a vertical UWVLC link in inhomogeneous environment is presented. Two system models are discussed, LOS and NLOS where the Tx and Rx are both located underwater. The performance is studied for a vertical link with gradient refractive index and attenuation profiles. The gradient profiles are approximated to stratified layers with calculated average optical properties. Crude to more accurate approximations were applied to resemble the gradient refractive index and attenuation profiles. Received BER and power are calculated for different profile approximations. Performance alterations are discussed for each of the approximate cases in comparison to the case of employing a homogeneous medium. To the best of our knowledge no similar approach has been previously addressed in literature. The value of this work lies in providing a means to accurate link budget calculations with consideration of underwater environment inhomogeneity. When discarding underwater inhomogeneity, an overestimation in the received power is obtained. Thus, precise link budget calculations presented in this work serve to correctly estimate the required transmission to satisfy the target quality-of-service.

This paper is organized as follows: In section II, inhomogeneous UW link parameters including attenuation and refractive indices are introduced. In section III, these parameters are utilized to model the inhomogeneous UW structure as N homogeneous layers. A geometrical optics background required for the link budget model is introduced, from which the mathematical model for received power follows. The model is then examined in detail. Finally, a numerical example is used to quantify the received power and BER for LOS and NLOS vertical UW links. Optimum Tx-Rx angular separation along with an optimum Tx orientation and half cone angle are obtained.

II. VERTICAL UW LINK PARAMETERS

Physical properties of UW environment vary, not only geographically, but with vertical depth from the sea-level [4], [13], [16], [17]. Below the sea-level, there is the euphotic zone, which is the topmost layer, followed by the dysphotic zone then the aphotic zone. The euphotic zone depth varies from 15m in coastal water to 200m in clear ocean water. This zone receives a sufficient amount of sunlight, thus characterized by relatively warm temperatures in addition to high chlorophyll concentration. Chlorophyll is a strong source of absorption - hence attenuation- of propagating light in that zone. At larger depths, the dysphotic zone is defined, which has a less amount of sunlight, thus suffers from lower temperature values than the euphotic zone. Further below, there exists the aphotic zone with almost no sunlight reaching it, thus suffers from a relatively low temperature compared to upper water layers. Since, each zone exhibits its unique physical characteristics, it thus requires a unique link budget model [4]. In this work, a generalized link budget model is proposed taking into account the above mentioned variations in optical parameters with depth. Hence, enabling performance evaluation of an UW link in different zones using only one link budget model at a given wavelength of operation (λ).

It is important to mention that the above optical and physical properties of water are spectral dependent. According to [18], seawater exhibits relatively low attenuation in the blue-green spectrum, which corresponds to the spectral window 450nm-550nm. However, typically longer wavelengths may be employed in UW optical communications to overcome the attenuation resulting from particles and dissolved organic materials. The attenuation of such particles is dominated by chlorophyll, which experiences a minimum attenuation near the green spectrum. Hence, in this work, λ is

chosen as 532nm to guarantee operating under minimum attenuation [15].

A. INHOMOGENEOUS EXTINCTION COEFFICIENT PROFILE

In general, total attenuation of light may be expressed as an extinction coefficient $c(\lambda)$, which relates to the attenuation and scattering coefficients; $\alpha(\lambda)$ and $\beta(\lambda)$, respectively, as follows [2], [4]:

$$c(\lambda) = \alpha(\lambda) + \beta(\lambda) \tag{1}$$

In literature it is typical to express $c(\lambda)$ with a single value at a given wavelength, which is a loose approximation due to the variations of $\alpha(\lambda)$ and $\beta(\lambda)$ with depth. The spectral dependence of light absorption arises from depth dependent properties of water molecules, suspended particles, dissolved salts and chlorophyll concertation [4], [13]. As for scattering, it is assumed in this work that the extinction coefficient is mainly affected by $\alpha(\lambda)$. This assumption is valid for open waters, where scattering is not of significant effect [4], [10].

Typical values of $c(\lambda)$ range from $0.3m^{-1}$ to $0.022m^{-1}$ from the sea-level downwards [13].

B. INHOMOGENEOUS REFRACTIVE INDEX PROFILE

According to the empirical formula in [16], UW refractive index n is dependent on T, P, S and λ as follows,

$$n(T, P, S, \lambda) = n_I + n_{II} + n_{III} + n_{IV}, \tag{2}$$

where,

$$\begin{aligned} n_I &= A_o + L_2 \cdot \lambda + \frac{LM_2}{\lambda^2} + \frac{LM_4}{\lambda^4} + \frac{LM_6}{\lambda^6} + T_1 \cdot T + T_2 \\ &\quad \cdot T^2 + T_3 \cdot T^3 + T_4 \cdot T^4 + TL \cdot T \cdot \lambda + T_2L \cdot T^2 \cdot \lambda \\ &\quad + T_3L \cdot T^3 \cdot \lambda, \\ n_{II} &= S_o \cdot S + S_1LM_2 \cdot \frac{S}{\lambda^2} + S_1T \cdot S \cdot T + S_1T_2 \cdot S \cdot T^2 \\ &\quad + S_1T_3 \cdot S \cdot T^3 + STL \cdot S \cdot T \cdot \lambda, \\ n_{III} &= P_1 \cdot P + P_2 \cdot P^2 + PLM_2 \cdot \frac{P}{\lambda^2} + PT \cdot P \cdot T \\ &\quad + PT_2 \cdot P \cdot T^2 + P_2T_2 \cdot P^2 \cdot T^2, \end{aligned}$$

and

$$n_{IV} = P_1S \cdot P \cdot S + PTS \cdot P \cdot T \cdot S + PT_2S \cdot P \cdot T^2 \cdot S$$

where the numerical constants in (2) are defined in [16], T is in ° Celsius, P in $dbar$, S in percent and λ is in nanometers. T, P and S exhibit different profiles with depth for different water types [16], [17], [19]. From [19], typical values of T and S with depth are in the ranges of 25° and 37% at the sea-level to 0° and 34% at the sea-bed for T and S, respectively. Pressure (P) increases by $10dbar$ every $\sim 10m$ depth in a linear relation [17]. By substituting the above values in (2), a refractive index range of 1.3413-1.3674 is obtained, where n increases with increasing depth, i.e., from sea-level downwards.

C. INHOMOGENEOUS MEDIUM AS STRATIFIED LAYERS

A homogeneous medium exhibits single values of $c(\lambda)$ and n. Hence, according to geometrical optics, light travels in such a

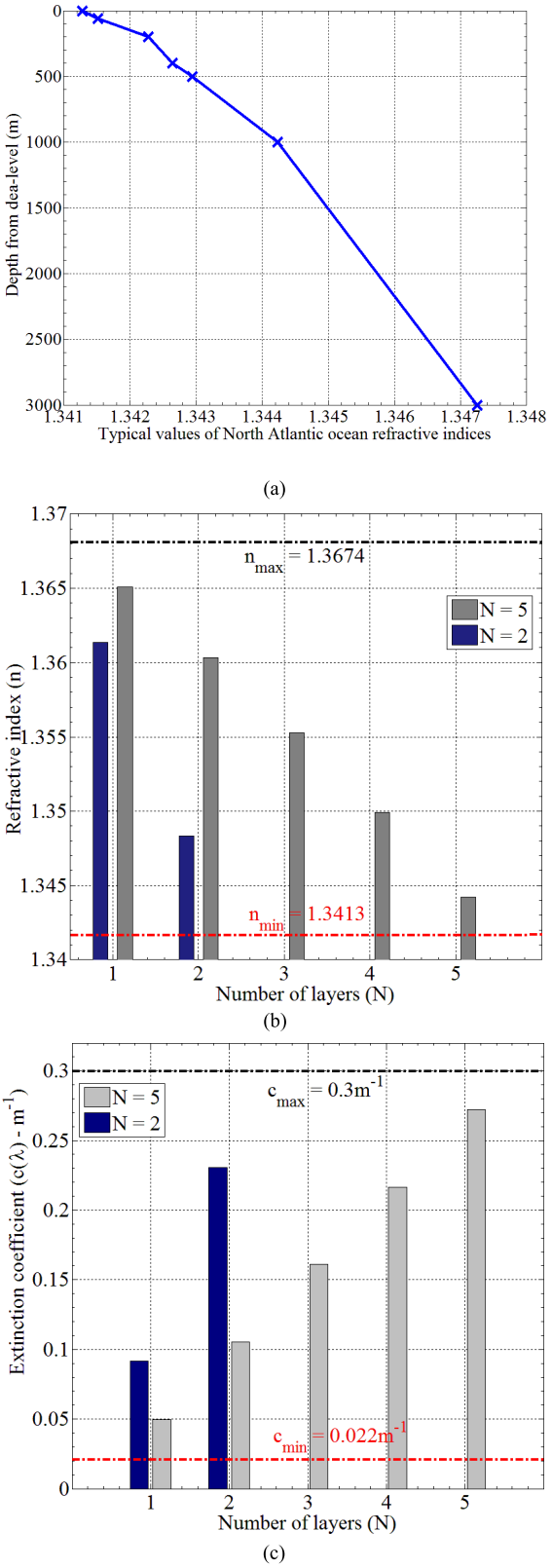

FIGURE 1. (a) Actual values of n versus depth of the North Atlantic Ocean [19]. (b) Approximate calculated values of n when representing its actual gradient profile by 5 and 2 layers, respectively. $N = 1$ refers to the bottom-most layer near the sea-bed. (c) Approximate calculated values of $c(\lambda)$ when representing its actual gradient profile by 5 and 2 layers, respectively. $N = 1$ refers to the bottom-most layer near the sea-bed.

medium in a straight line with power loss obeying Beer's law: $P = P_o e^{-c(\lambda).L}$, where P is the power at a traveled distance L and P_o is the initially transmitted power [2]–[4].

On the other hand, in a medium with a gradient $c(\lambda)$ and n profile, light is not expected to behave in the same manner. Studying light propagation in a gradient profile might include complex analysis. Hence, for simplicity, in this work, the gradient profile is approximated to N stratified layers. A similar approach is adopted in studying optical fibers with gradient refractive index profiles [20]. However, this is the first time this approach is applied to study underwater inhomogeneous nature. A typical behaviour of n versus depth in is shown in Fig. 1(a). Such gradient inhomogeneous profile may be treated as stratified layers N with distinct values of $c(\lambda)$ and n as shown in Fig. 1(b) and (c). All layers are assumed to be of equal thicknesses, with each having distinct values of $c(\lambda)$ and n. These distinct average values are obtained by average linearization of $c(\lambda)$ and n profiles. Maximum and minimum typical values of $c(\lambda)$ are $0.3m^{-1}$ and $0.022m^{-1}$, respectively [13], whereas maximum and minimum values of n are calculated from (2); $1.3413 - 1.3674$, at $\lambda = 532nm$.

Approximate linearized values of $c(\lambda)$ and n are shown in Fig. 1(b) and (c) for two cases where their gradient profiles are represented by two and five layers. Naturally, as N increases, more accurate profiles are obtained. However, utilizing a small number of layers is shown in Fig. 1(b) and (c) is only the purpose of illustrating the idea. In section IV, a significantly larger N is used for better accuracy along with a comparison of errors arising due to changing N and deduction of the optimum number of layers N_{opt} for gradient profile representation.

III. SYSTEM LINK BUDGETS

Two link budget scenarios for LOS and NLOS –shown in Fig. 2 - are assumed. A mathematical model of the received power is derived for each scenario with consideration of the inhomogeneous nature of UW medium. The model is further used to evaluate the performance of LOS and NLOS links in Fig. 2.

A. THEORETICAL BACKGROUND

As earlier illustrated, the inhomogeneity of $c(\lambda)$ and n are represented by gradient profiles adopted from typical data in [13], [16], [17], and [19]. A typical behaviour of n versus depth is shown in Fig. 1(a). Such gradient inhomogeneous profile may be treated as stratified layers N with distinct values of $c(\lambda)$ and n as shown in Fig. 1(b) and (c).

The propagation of light in a stratified medium may be explained by Fresnel's law [21]. When light strikes an interface between two media with different n, it undergoes partial transmission/refraction and partial reflection. As a matter of fact, light loses its polarization while propagating in a scattering medium such as UW environment. It is established that transmission and reflection of unpolarized light are expressed in terms of transmission and reflections of extreme polarization states, i.e., ($s-$) perpendicular and ($p-$) parallel polarized lights.

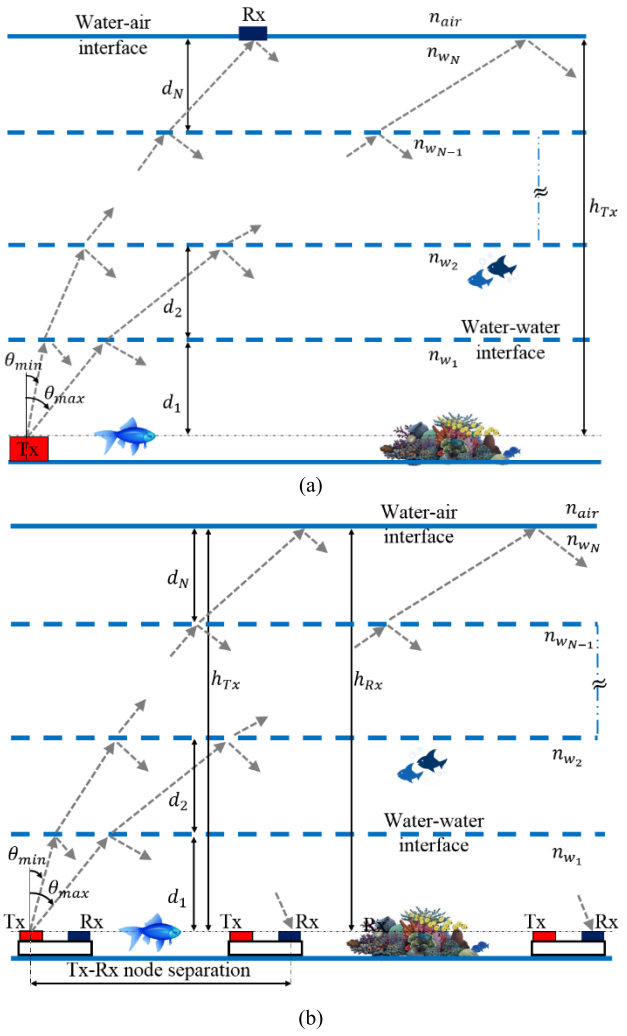

FIGURE 2. (a) LOS link scenario under study. (b) NLOS link scenario under study.

Hence, light striking all interfaces is considered totally unpolarized with power reflectivity of $R_{i1,2} = \frac{1}{2}(R_{s_{i1,2}} + R_{p_{i1,2}})$, where $R_{s,p}$ are power reflectivities of s- and p- polarizations, respectively, and $i_{1,2}$ denote the 1st and 2nd interfaces as illustrated in Fig. 2. According to Fresnel, a light incident from medium I on another medium II, undergoes partial reflection, $R_{s,p}$ at the $I - II$ interface given by [21]:

$$R_{s_{I-II}} = \left[\frac{n_I \cos(\theta_I) - n_{II} \cos(\theta_{II})}{n_I \cos(\theta_I) + n_{II} \cos(\theta_{II})}\right]^2 \quad (3)$$

$$R_{p_{I-II}} = \left[\frac{n_I \cos(\theta_{II}) - n_{II} \cos(\theta_I)}{n_I \cos(\theta_{II}) + n_{II} \cos(\theta_I)}\right]^2 \quad (4)$$

where θ_I and θ_{II} are the incident angles and transmission angles in media I and II, respectively. The transmission angle θ_{II} is related to θ_I by Snell's law: $n_I sin\theta_I = n_{II} sin\theta_{II}$. Thus, power transmissions at the $I - II$ interfaces are given by: $T_{s_{I-II}} = 1 - R_{s_{I-II}}$, for $s-$ polarization and $T_{p_{I-II}} = 1 - R_{p_{I-II}}$ for $p-$ polarization. Hence, the resulting transmission of unpolarized light is: $T_{i1,2} = \frac{1}{2}(T_{s_{i1,2}} + T_{p_{i1,2}})$.

Total internal reflection (TIR) phenomenon may take place at the incidence medium I when it is denser than the transmission medium II; $n_I > n_{II}$. TIR occurs when θ_I surpasses the critical angle at the $I - II$ interface, which is defined by Snell's law as [21]:

$$\theta_c = sin^{-1}\left(n_{II}/n_I\right) \tag{5}$$

During TIR, all incident light reflects back from the $I - II$ interface.

In the link models of interest in this work (Fig. 2), air (n_{air}) is less dense than seawater, and seawater gets denser with increasing depth, i.e., $n_{air} < n_{w_N} < n_{w_{N-1}} < \cdots < n_{w_1}$ [16]. The refractive indices $n_{w_{1,2\ldots N}}$ are the indices of stratified layers used to resemble the inhomogeneous UW nature as shown in Fig. 2. Hence, if the light propagates from the sea-bed upwards, i.e., from denser to less dense medium, TIR is anticipated to take place at all interfaces of Fig. 2. By applying (5), the critical angles at all w-w and w-air interfaces can be expressed as follows,

$$\theta_{c,ww} = sin^{-1}\left(\frac{n_{w_{i+1}}}{n_{w_i}}\right) \tag{6-a}$$

$$\theta_{c,wa} = sin^{-1}\left(\frac{n_{air}}{n_{w_N}}\right) \tag{6-b}$$

B. LINK BUDGET MODELS

Power at the Rx's end is basically quantified through multiplying the transmitted power, Tx and Rx gains, and the path loss encountered by the propagation of the light signal. Path loss in an inhomogeneous medium modeled as N stratified layers is mainly caused by: 1) attenuations (γ_i), following Beer's law [2]-[4] given by, $\gamma_i = \exp(-c_i(\lambda) \cdot L_i)$, where $c_i(\lambda)$ and L_i are the extinction coefficient and the distance traveled by light in layer i, respectively, and $i = 1, 2, \ldots, N$, 2) partial reflections and/or transmissions at water-air and all water-water interfaces. Partial reflections and transmissions are expressed as power reflection and transmission coefficients defined in the previous section (III-A).

1) LOS MODEL

The link model in Fig. 2(a) is considered, in which the Tx is located at the sea-bed at a depth of h_{Tx} from the sea-level (water-air interface). The Rx, on the other hand, is located at the sea-level at a height of $h_{Rx} = 0$ from the water – air interface as shown in Fig. 2(a). The Tx is primarily directed upwards, thus emitting a light cone with an inner angle $\theta_{min} = 0°$ and an outer angle of $\theta_{max} = 68°$ [10]. The Rx(s) are positioned at angular separation(s) (θ) from the Tx, with $\theta_{min} < \theta < \theta_{max}$. The metric separation between the Tx and the Rx may be denoted by: $(h_{Tx} + h_{Rx})/cos\theta$. All water-water (w-w) and water-air (w-a) interfaces are assumed to be smooth surfaces, hence, transmission and/or reflection angles shall not deviate from those theoretically calculated by Snell's law [10], [18].

Light propagation from the Tx to the Rx may be elaborated in terms of geometric optics as follows. The received power is the fraction of light capable of crossing all the w-w interfaces between the Tx and Rx without undergoing TIR. That is, for $h_{Rx} = 0$, only light with $\theta_{min} < \theta < \min(\theta_{c,ww})$ will be able to reach the Rx. Whereas for $h_{Rx} > 0$, a smaller fraction of light will be able to cross all the w-w as well as the w-a interfaces; i.e. only light with $\theta_{min} < \theta < \theta_{c,wa}$ shall reach the Rx, where $\theta_{c,wa} < \min(\theta_{c,ww})$, as from (6).

The Rx's aperture size (A_{Rx}) is usually small compared to the distance between the Tx and the Rx. Therefore, the link budget model of the system in Fig. 2(a) may be mathematically modeled as,

$$P_r = P_t \cdot A_{Rx} \cdot \cos\theta \cdot \eta_{Tx} \cdot \eta_{Rx} \cdot L(\theta) \tag{7}$$

where $L(\theta)$ is the path loss per the illuminated area A_L, illustrated hereafter. Light traveling from the Tx in the sea-bed to the Rx at the sea-level passes through N layers of equal thicknesses d_i as shown in Fig. 2(a). Each layer has a distinct extinction coefficient $c_i(\lambda)$ and a different refractive index value n_{w_i}. Light enters each layer with a transmission angle θ_i (easily calculated by direct application of Snell's law), experiences attenuation of $\gamma_i = \exp(-c_i(\lambda) \cdot L_i)$, where $L_i = d_i/cos\theta_i$. Generally, each layer i has an arbitrary thickness d_i that is determined according the underwater refractive index profile. It experiences further attenuation as it is partially transmitted into layer $i + 1$, hence multiplied by $T_{i,i+1}$. The above illustration may mathematically be expressed as,

for $h_{Rx} = 0$:

$$L(\theta) = \begin{cases} \dfrac{1}{A_L} \exp\left\{-\displaystyle\sum_{i=1}^{N} \frac{d_i \cdot c_i(\lambda)}{\cos(\theta_i)}\right\} \cdot \displaystyle\prod_{i=1}^{N} T_{i,i+1}; \\ \qquad for\ \theta_{min} \le \theta < \min(\theta_{c,ww}), & (8a) \\ Zero \quad for\ \min(\theta_{c,ww}) < \theta \le \theta_{max}, & (8b) \end{cases}$$

The light cone emitted by the source illuminates the sea-level with an annular surface area (A_L) that is generally calculated as $A_L = 2\pi R(H_{max} - H_{min})$. The perpendicular distance between the Tx and Rx is R and $H_{min,max} = 1 - cos\theta_{min,max}$. The angles $\theta_{min,max}$ are the inner and outer angles of the Tx's light cone as previously mentioned. Therefore, the annular area in (7) and (8) may be given by:

$$A_L = 2\pi\,(h_{Tx} + h_{Rx})^2\,(cos\theta_{min} - cos\theta_{max}) \tag{9}$$

2) NLOS MODEL

The NLOS link model considered herein is shown in Fig. 2(b). It is a point-to-multipoint system in which the Tx and the Rx(s) are at depths h_{Tx} and h_{Rx}, respectively, from the sea-level (w-a interface). The Tx is initially pointed upwards such that it emits a light cone with inner angle and outer angles of $\theta_{min} = 0°$ and $\theta_{max} = 68°$, respectively. The Rx(s) are positioned at angular separation(s) (θ) from the Tx, with$\theta_{min} < \theta < \theta_{max}$. The metric separation between the Tx and the Rx(s) – which may be denoted here by Tx-Rx node separation- is given by: $(h_{Tx} + h_{Rx})tan\theta$. Again,

all w-w and w-a interfaces are assumed to be smooth surfaces, therefore, transmission and/or reflection angles shall not diverge from those theoretically calculated using Snell's law [18], [21].

For the link shown in Fig. 2(b), both the Tx and the Rx(s) are assumed to rest on the sea-bed at the same depth. The trip of light from the Tx to the Rx(s) may be explained in the light of geometrical optics as follows. Recall the fact that bottom water layers are denser than the upper ones, and in turn denser than air. Consequently, light traveling from the Tx upwards may be categorized according to its angleθ into three groups; 1) $\theta_{min} < \theta < \theta_{c,wa}$, 2)$\theta_{c,wa} < \theta < \min(\theta_{c,ww})$ and $\min(\theta_{c,ww}) < \theta < \theta_{max}$. The first group undergoes partial reflection at the w-a interface, whereas the second group experiences TIR at the same interface. The third group references the TIR possibility at each w-w interface if $\theta_{c,w_iw_{i+1}} < \theta < \theta_{max}$, where $\theta_{c,w_iw_{i+1}}$ is the critical angle at $i - i + 1$ interface. This case is not applicable except for Tx orientations where $\theta_{max} > \min(\theta_{c,ww})$. Mathematical explanation of the above groups is given by 10(a-d), respectively, with the third group is represented by both 10(c-d). It is important to mention herein, that partial reflections at w-w interfaces in cases (1) and (2) may be conveniently neglected. This attributes to the small difference in values between n_i and n_{i+1}. This results in relatively large transmitted fraction of light, hence a significantly minor reflected fraction according to (3)-(4).

As previously mentioned, the Rx's aperture size (A_{Rx}) is typically small in comparison to the distance between the Tx and the Rx. Hence, the link budget model of the system in Fig. 2(b) may be mathematically modeled by (7), where $L(\theta)$ is the path loss per illuminated areas $A_{L1,2}$ - illustrated hereafter- and is expressed as:

$$
L(\theta) = \begin{cases}
\dfrac{1}{A_{L1}} \exp\left\{-2\sum_{i=1}^{N} \dfrac{d_i.c_i(\lambda)}{\cos(\theta_i)}\right\} \cdot \prod_{j=1}^{N-1} T_{j,j+1} \cdot R_{w,air} \cdot \prod_{q=1}^{N-1} T_{q+1,q}; \\
\qquad for\ \theta_{min} \le \theta < \theta_{c,wa} \qquad (10a) \\
\dfrac{1}{A_{L1}} \exp\left\{-2\sum_{i=1}^{N} \dfrac{d_i.c_i(\lambda)}{\cos(\theta_i)}\right\} \cdot \prod_{j=1}^{N-1} T_{j,j+1} \cdot \prod_{q=1}^{N-1} T_{q+1,q}; \\
\qquad for\ \theta_{c,wa} < \theta \le \min(\theta_{c,ww}) \qquad (10b) \\
\dfrac{1}{A_{L2_g}} \left[\exp\left\{-2 \times \left(\sum_{i=1}^{N} \dfrac{d_i.c_i(\lambda)}{\cos(\theta_i)} - \sum_{k=N}^{g} \dfrac{d_k.c_k(\lambda)}{\cos(\theta_k)}\right)\right\} \times \prod_{j=1}^{g-1} T_{j,j+1} \cdot \prod_{q=1}^{g-1} T_{q+1,q}\right]_{g=N,N-1.....,3}; \\
\qquad for\ \theta_{c,w_{g-2},w_{g-1}} < \theta \le \theta_{c,w_{g-3},w_{g-2}} \qquad (10c) \\
\dfrac{1}{A_{L2_g}} \left[\exp\left\{-2 \times \left(\sum_{i=1}^{N} \dfrac{d_i.c_i(\lambda)}{\cos(\theta_i)} - \sum_{k=N}^{g} \dfrac{d_k.c_k(\lambda)}{\cos(\theta_k)}\right)\right\}\right]_{g=2} \\
\qquad for\ \theta_{c,w_1,w_2} < \theta \le \theta_{max} \qquad (10d)
\end{cases}
$$

where $d_i = h_{Tx}/N$ is the thickness of a single water layer and N is the number of layers starting from the sea-bed upwards as in Fig. 2(b)

As previously explained, the area illuminated via a light cone is expressed as a spherical sector with annular surface area of $2\pi R(H_{max} - H_{min})$, where R is the perpendicular distance between the Tx and the Rx, and $H_{min,max} = 1 - cos\theta_{min,max}$. The angles $\theta_{min,max}$ are the inner and outer angles of the Tx's light cone as illustrated previously. Therefore, the annular areas in (10) may be expressed as:

$$A_{L1} = 2\pi (h_{Tx} + h_{Rx})^2 (cos\theta_{min} - cos\theta_{max}) \qquad (11a)$$

$$A_{L2_g} = 2\pi \left(\sum_{i=1}^{N} 2d_i - \sum_{k=N}^{g} 2d_k\right)_{g=N,N-1,...,2} \times (cos\theta_{min} - cos\theta_{max}) \qquad (11b)$$

C. BER CALCULATIONS

P_r calculated using (7) through (11) is used to evaluate the system performance defined in terms of BER. A BER calculation formula is adopted from [10]. In this work, the intensity modulation technique is assumed to be on-off keying (OOK) with direct detection method (DDM). OOk-DDM is a well-established technique and vastly adopted in the literature [2]–[4], [10]. Light reception is assumed to be achieved by photon counting with a single photon avalanche detector. Hence, the photon arrival rate (R_p) at the Rx within a Rx time slot (t_{Rx}) is [10]:

$$R_p = \frac{1}{t_{Rx}} \left(\frac{P_r}{R_B}\right) \frac{\eta_c}{h\nu} \qquad (12)$$

where the data rate is R_B, the detector counting efficiency is η_c, the received power (P_r) is calculated from (7) through (11) and the energy of a single photon is $h\nu$ (h is Planck's constant and ν is the operating frequency $= 2\pi/\lambda$). Therefore, from [10], the BER may be approximately expressed as:

$$BER = \frac{1}{2} erfc\left[\frac{R_1 t_{Rx} - R_o t_{Rx}}{\sqrt{2}(\sqrt{R_1 t_{Rx}} + \sqrt{R_o t_{Rx}})}\right] \qquad (13)$$

where $R_1 = R_D + R_{BG} + R_p$ and $R_o = R_D + R_{BG}$. The sources of noise are assumed to be dark counts and background illumination, represented as R_D and R_{BG}, respectively. The error function $erfc(x)$ is defined as: $erfc(x) = \frac{2}{\pi} \int_x^\infty \exp(-x^2)dx$.

In the upcoming section, a numerical example is introduced for quantifying the received power and BER for the systems in Fig. 2 at distinct Rx angular positions and Tx average powers. The effect of varying the Tx orientation angle along with the width of the transmitted light cone on the link budget model is presented. Typical UW parameter values are adopted from [10], [13], [16], [17], and [19].

IV. RESULTS AND DISCUSSION

The modeled links are shown in Fig. 2. In both, the Tx is placed in the sea-bed (denser water) with depth h_{Tx} from the sea-level. For the LOS system in Fig. 2(a), the Rx is located at the sea-level with $h_{Rx} = 0$. On the other hand, the Rx(s)

in the NLOS system of Fig. 2(b) are placed in the sea-bed at a depth of $h_{Rx} = h_{Tx}$. The Tx is a laser source operating at 532 nm. The Tx is initially pointed upwards, such that it produces a light cone with $\theta_{min} = 0°$ and $\theta_{max} = 68°$, with an average transmission power (P_t) of 1W. It exhibits an efficiency $\eta_{Tx} = 0.9$. As for the Rx, it has an aperture size (A_{Rx}) of $0.01m^2$ and an efficiency $\eta_{Rx} = 0.9$. The Rx is chosen to be omni-directional or self-aligned to guarantee angle tolerant reception.

An $N-$layer system composed of N homogenous stratified layers is used to model the inhomogeneous nature of the underwater environment. Typical values of refractive indices and extinction coefficients at different depths are used to study the effect of their variations on the LOS and NLOS links performance. The refractive index n and the extinction coefficient $c(\lambda)$ values at $\lambda = 532nm$ range between $1.34213 - 1.3674$, and $0.3m^{-1}0.022m^{-1}$, as calculated from (2) and adopted from [13], respectively. Recall the fact that the deeper the water, the more dense it is and the less attenuating it becomes. All layers are assumed to be equally distant with thickness $d = h_{Tx}/N$.

The links in Fig. 2 are tested under data transmission rate of ($R_B = 0.5$Mbps). The noise contributors are presumed to be; 1- a background noise ($R_{BG} = 2MHz$) and dark photon counts ($R_D = 2MHz$). The counting efficiency of the Rx detector is ($\eta_c = 16$). The forward error correction (FEC) limit is set as 10^{-3}.

A. LOS INHOMOGENEOUS LINK PERFORMANCE

The received power (P_r) and BER are calculated from the mathematical model in (7)-(9) and (12)-(13) using the above mentioned parameters. In the upcoming results, the Rx is assumed to be located at the sea-level or slightly below, i.e. $h_{Rx} = 0$. This assumption guarantees that the Tx-Rx link is completely underwater. From Fig. 2(a), the link metric length may geometrically be given by $h_{Tx}/cos\theta$, where $0° \leq \theta \leq 68°$ is the angular Rx position as in Fig. 2(a). The angular Rx position θ may be defined as the angle between the normal on the receiver's plane and the received light. In this work, the link performance is studied versus θ rather than $h_{Tx}/cos\theta$, for the sake of generalizing current results for arbitrary h_{Tx}.

Fig. 3 studies the impact of approximating the inhomogeneous underwater medium with different number of layers N in comparison to the homogeneous assumption ($N = 1$). For each N, the typical refractive index and extinction coefficient values are used to calculate average n_{w_i} and $c_{w_i}(\lambda)$ for each layer i. These average values are obtained through: 1- linearization of $c(\lambda)$ and n gradient profiles, 2- averaging these linearized values according to the number of layers adopted in the model as illustrated previously in Fig. 1. From Fig. 3(a), it is obvious that as N increases, the BER curve though preserves its behaviour, the angular Rx position θ at FEC of 10^{-3} decreases. This decrease becomes unnoticeable at larger values of N; i.e., 50 and 100. This dictates

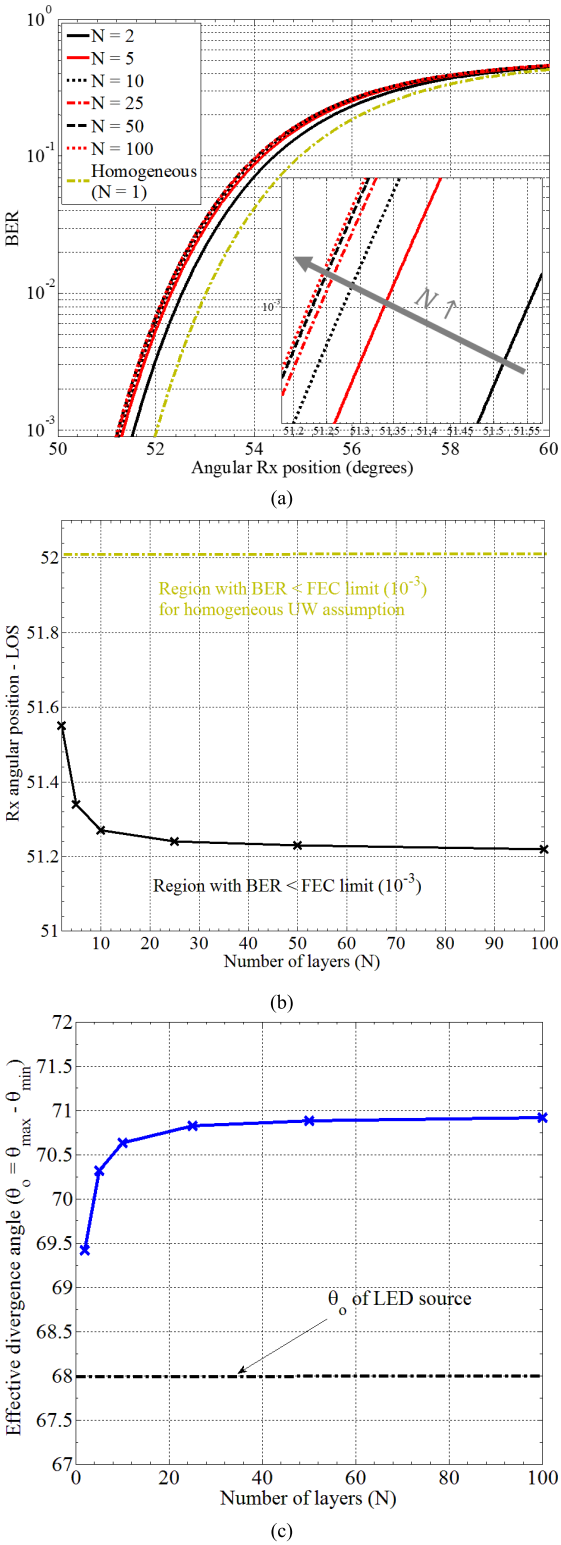

FIGURE 3. (a) BER versus Tx-Rx angular separation – LOS system in Fig. 2(a)-at different approximations of the gradient profiles of n and $c(\lambda)$. Inset: Zoom in around the FEC limit (10^{-3}). (b) Maximum Rx angular positions (at BER = FRC limit (10^{-3})) for the LOS system in Fig. 2(a). The region below the curve indicates the Rx angular positions from Tx that guarantee BER < FEC. (c) Effective divergence angle of light at the sea-level due to variations in N. Divergence angle of Tx source = 68°.

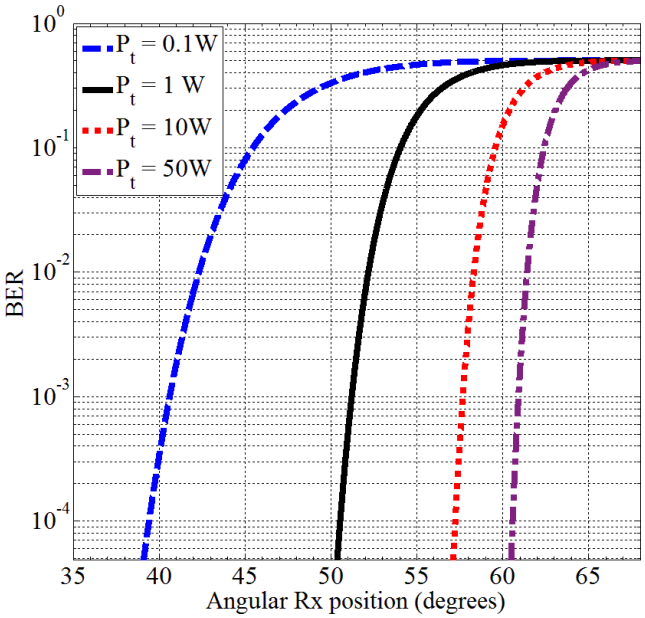

FIGURE 4. Effect of changing P_t on maximum acceptable angular Rx position for LOS system in Fig. 2(a). $N = 50$.

that the approximation of underwater inhomogeneous model with only 2 layers is a rough approximation. Although it may well indicate the overall behaviour, but fails to offer accurate measures for the furthest possible Rx position as illustrated in Fig. 3(b). Fig. 3(b), shows the maximum angular Rx position θ anticipated from using different values of N. It is important to note herein that although the differences in angular Rx positions θ may seem relatively small (in order of decimals of degrees), they become more pronounced as the depth of the Tx from the sea-level increases. The overestimation of the maximum angular Rx position θ due to applying the homogeneous UW assumption ($N = 1$) is shown in Fig. 3(b) as well.

The overestimated angular Rx position θ at lower N values may be attributed to neglecting multiple light refractions at water layers with different n. In Fig. 3(c), the deviation of θ of the emitted light cone is shown for different values of N. As N increases, the propagating light faces more interfaces, hence more deviations according to Snell's law [21]. This causes an elongated path for light, thus encountering more losses and in turn causing the BER to increase at lower θ. As N further increases, light experiences minimal deviations, which ensures the previous deduction that $N = 50 - 100$ offers a good approximation of the typical gradient profiles of n and of $c(\lambda)$.

In Fig. 4, the BER behaviour is examined for different angular Rx positions θ, where $0° \leq \theta \leq 68°$ at different P_t. The average transmitted power P_t ranges from 0.1W to 50W. From Fig. 4, it is evident that as P_t increases, the Rx may be placed at a larger angular positions θ. By increasing P_t 10 times (from 0.1W to 1W), the maximum θ (equivalent to FEC limit of 10^{-3}) increases by 10°. But, further increasing P_t from 1W to 10W does not result except in a 5° increase in maximum θ. This is expected as the increase in P_t may compensate the optical path losses encountered by the transmitted data at lower values of θ. However, at larger values, the optical path becomes longer, hence subjected to an amount of attenuation that surpasses the ability of P_t to compensate it.

B. NLOS INHOMOGENEOUS LINK PERFORMANCE

The mathematical model in (7) and (10) through (13) is used to quantify the received power (P_r) and BER using the previously mentioned parameters. As shown in Fig. 2(b), different Tx and Rx nodes are located in the sea-bed at the same depth, such that $h_{Rx} = h_{Tx}$. The node separation distance may geometrically is given by $(h_{Tx} + h_{Rx})tan\theta$, where $0° \leq \theta \leq 68°$ is the angular Rx position as in Fig. 2(b). In this work, BER curves are plotted versus the angular Rx position θ rather than $(h_{Tx} + h_{Rx})tan\theta$. This helps in easier interpretation of the results for arbitrary h_{Tx}.

Fig. 5 shows the effect of underwater inhomogeneous medium modeling by two to hundred stratified layers in comparison to homogeneous UW assumption ($N = 1$). Before diving into evaluating the link approximation model, it is important to understand the BER behaviour for the NLOS link in Fig. 2(b). The BER curves in Fig. 5(a) may be divided into three regions. The first region from the left, resembles a conventional BER behaviour similar to a LOS link where BER increases with increasing Tx-Rx separation. This takes place till $\theta \sim 40°$ where BER starts to decrease and a clear dip is observed. This dip region appears centered around $\theta \sim 47°$, which indicates light transmission at $\theta \sim \theta_{c,wa}$. This is expected due to TIR at the w-a interface, where light power totally reflects from the w-a interface without being reduced by partial reflection. The third region is at θ further beyond $\theta_{c,wa}$. In this region, the optical signal travels a relatively longer distance due to beam refractions at w-w interfaces, thus experiences higher attenuation. These attenuations cannot be compensated by TIR of the transmitted power, hence the BER increases again. Consequently, there exists two regions that satisfy the FEC limit.

As for the effect of Nlayer approximation, it is obvious that similar to the LOS case in Fig. 3(a), the BER curve in Fig. 5(a) preserves its behaviour but does not give an accurate estimation of acceptable angular Rx position θ. $N = 1, 2$ appear to be a rough approximation, whereas $N = 50$ seems to be the least number of layers for accurate performance estimation for the two regions satisfying the FEC limit as appears in Fig. 5(b).

In Fig. 6, the BER behaviour is observed at different angular Rx positions θ, where $0° \leq \theta \leq 68°$ at different P_t. The average transmitted power P_t ranges from 0.1W to 50W for the same total perpendicular Tx depth as in LOS for fair comparison ($h_{Tx_{LOS}} = 2h_{Tx_{NLOS}}$). This is because, in NLOS link, the light goes form the Tx to the sea-level and then back to the Rx. From Fig. 6, it is clear that $P_t = 0.1W$ fails to accommodate for the optical path losses in the NLOS

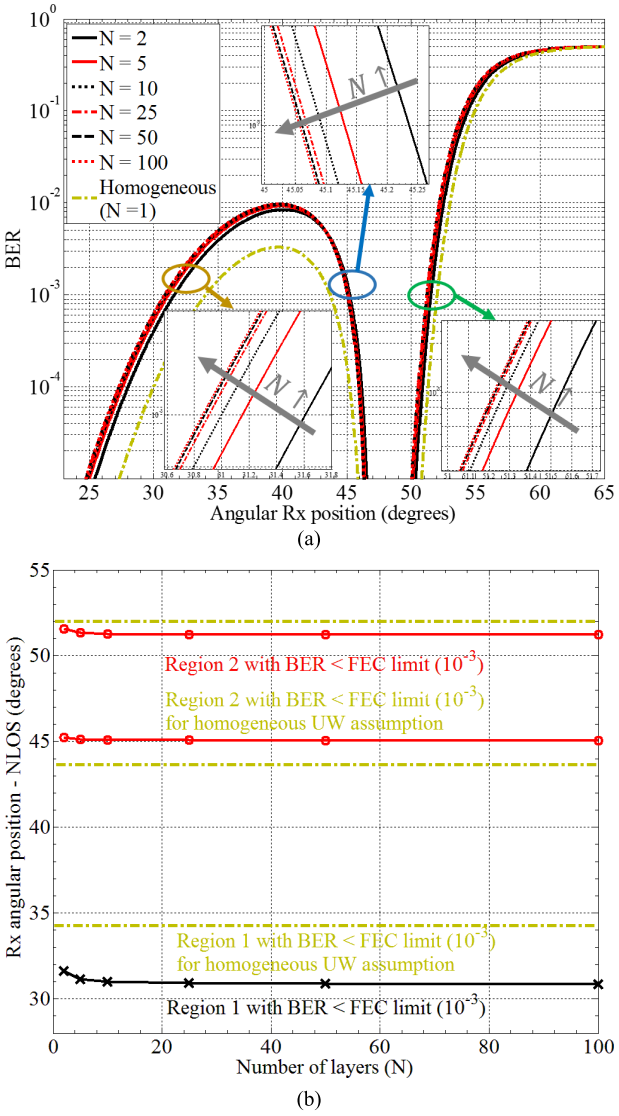

FIGURE 5. (a) BER versus Tx-Rx angular separation – NLOS system in Fig. 2(b) -at different approximations of the gradient profiles of n and $c(\lambda)$. Insets: Zoom in around the FEC limit (10^{-3}) for shown regions in ellipses. (b) Maximum Rx angular positions (at BER = FRC limit (10^{-3})) for the NLOS system in Fig. 2(b). Two regions satisfy BER < FEC; between the two upper lines, and below the bottom-most line.

link and appears to be inappropriate for the system of study. As P_t further increases, to 10W and 50W, it recovers the optical path losses at smaller θ allowing the Rx to be placed at a larger angular positions θ. The BER behaviour at large values of P_t resembles that of LOS in Fig. 4 and at larger values of θ, the optical path becomes longer, hence subjected to an amount of attenuation that exceeds the ability of P_t to compensate it.

C. ROUGH APPROXIMATIONS OF UNDERWATER MEDIUM

As previously illustrated, light propagation in an inhomogeneous medium leads to expected performance deviations from its counterpart in a homogeneous medium. This is due to n and $c(\lambda)$ variations as explained previously. As the number of layers N used to model the medium increases, a closer n and $c(\lambda)$ profiles are resembled. From the above results, $N = 50 - 100$ is proved to be sufficient for this purpose.

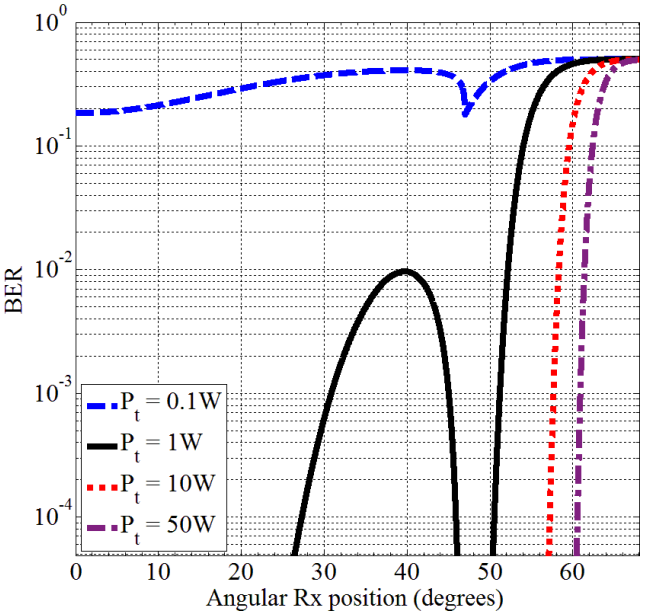

FIGURE 6. Effect of changing P_t on maximum acceptable angular Rx position for NLOS system in Fig. 2(b). $N = 50$.

In this section, a rough approximation model of two layers is introduced. This simple model may be less accurate, however, it gives a very close estimation to $N = 50-100$ models. The proposed rough approximation model, as named herein, is a bilayer model. The layers exhibit refractive indices of n_{w_1} and n_{w_2} given by maximum and minimum values of (2), respectively, at $\lambda = 532nm$ for S, T and P profiles previously employed.

The extinction coefficient for both layers is approximated as $c_{avg} = [max\,(c\,(\lambda)) + \min(c(\lambda))]/2$.

The adequacy of this rough approximation model is shown in Fig. 7. LOS and NLOS systems of Fig. 2 are modeled using stratified 50 layers, in addition to rough bilayer model as illustrated above. Good agreement of results is clear. The BER < FEC regions shift is in order of 0.1°, which is less than that obtained for a small N in Fig. 3(b) and 5(b).

It is worth mentioning here that this rough approximation is adequate for LOS systems at any Tx rotation, however, for NLOS systems at specific Tx rotations as discussed in section *IV-D*.

D. TX ROTATION IMPACT

The impact of Tx rotation on the LOS and NLOS systems of Fig. 2 is studied and introduced in Fig. 8. The initial Tx position is considered to be pointed upwards facing the sea-level; that is rotated with a central angle of zero ($\theta_{central} = 0°$). The Tx is further rotated with $\theta_{central} = 5°$, 10°, 15° and 20°, but preserving its divergence angle 68° in all these cases. BER values are calculated from (13) for different Rx angular positions (θ). For the Tx in this work

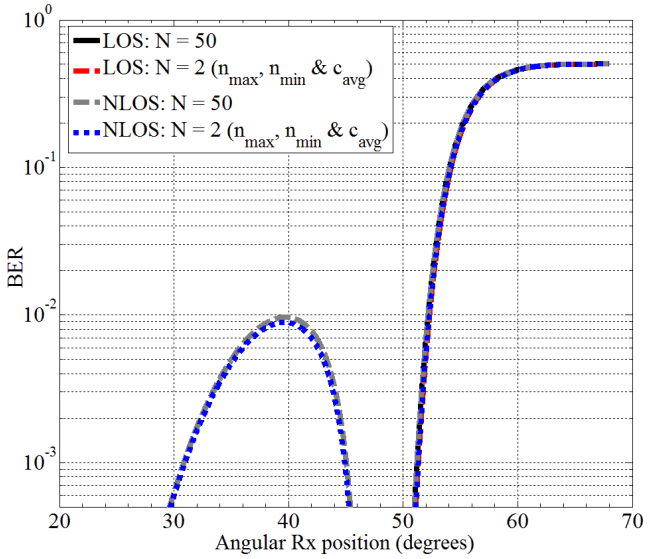

FIGURE 7. **Proposed rough approximation versus $N = 50$ layer model for LOS and NLOs systems of Fig. 2. Tx is pointed upwards towards the sea-level.**

with divergence angle of 68°, the θ_{c,ww_i} -which is in the range of ∼79° - shall fallout from the incident light cone. As the Tx is rotated and $\theta_{central}$ increases, θ_{c,ww_i} eventually falls into the incident light cone. Thus, at angles greater than θ_{c,ww_i}, TIR takes place at different w-w interfaces. For the LOS case, this prevents power from crossing the i^{th} interface. Hence, P_r is zero as deduced from (8b), which results in an increasing BER at angular Rx positions beyond θ_{c,ww_i}. As illustrated in Fig. 8(a), as the Tx inclination further increases, less power is expected at the same Rx positon. From Fig. 8(a), if a FEC limit of 10^{-3} is adopted, then a rotation of 0° shall result in a maximum angular Rx position of ∼ 51.23° which decreases to ∼49.9° at Tx orientation of 20°. Hence for LOS vertical links, the optimum Tx rotation is to be pointed upwards facing the sea-level; i.e with $\theta_{central} = 0°$ to guarantee the best possible link performance.

As for the NLOS case, at angles exceeding θ_{c,ww_i}, TIR is inevitable at different w-w interfaces. From θ_{c,ww_i} calculations, it appears that θ_{c,ww_i} between upper layers is less than between bottom layers. Hence, light transmitted with $\theta_{c,ww_{i-1}} < \theta < \theta_{c,ww_i}$, shall undergo TIR reflection at the ith interface. This takes place at each interface from sea-level downwards with P_r mathematically expressed by (10c)-(10d). Undergoing TIR at any of the interfaces below the sea-level the optical signal thus travels a shorter optical path $2(\sum_{j=1}^{j=i} d_j)/cos\theta$, rather than $2(N.d)/cos\theta$, where N is the total number of layers and $i < N$. Hence it faces less attenuation, which results in an increase in P_r and consequently a decrease in the BER as seen in Fig. 8(b). This case is unpronounced except at $\theta_{central}$ beyond 15° as shown in Fig. 8(b). The inset in Fig. 8(b) shows BER fluctuations at $\theta > \theta_{c,ww_i}$. These fluctuations are expected since at TIR at the i^{th} interface, light travels an optical path of $2(\sum_{j=1}^{j=i} d_j)/cos\theta$ as pointed out

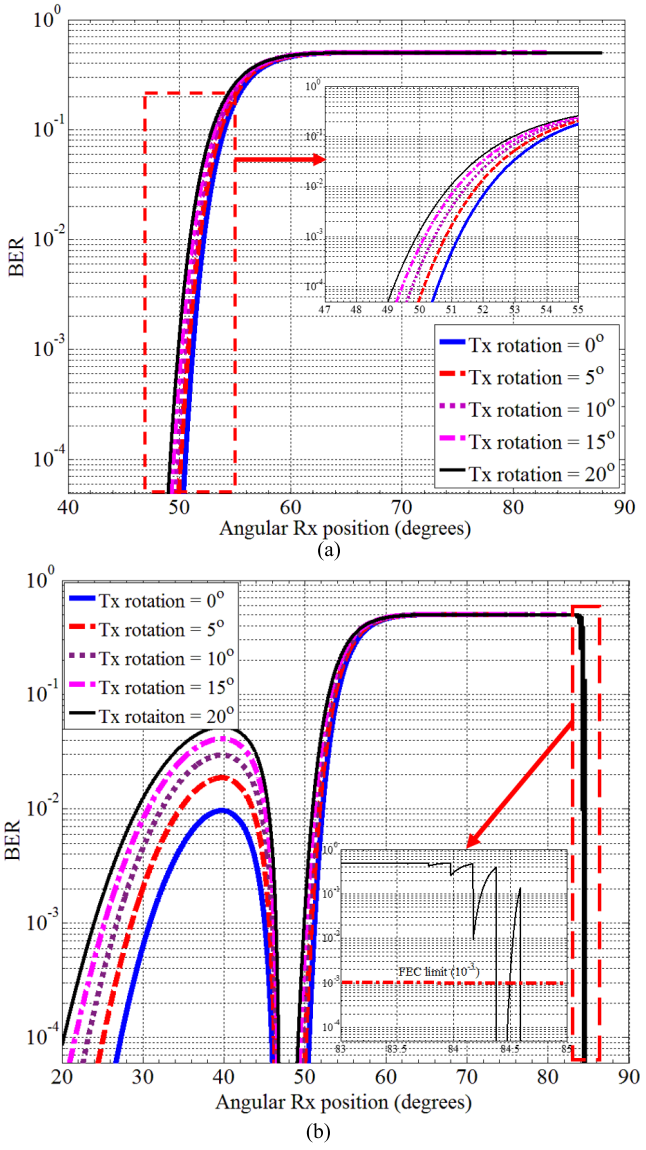

FIGURE 8. **(a) Effect of Tx rotation in NLOS system in Fig. 2(a), $N = 50$. (b) Effect of Tx rotation in NLOS system in Fig. 2(b), $N = 50$.**

previously. However, as θ increases, the denominator $cos\theta$ decreases, causing an increase in the optical path, which in turn causes an increase in the expected BER. This keeps happening till θ exceeds the critical angle of the $(i-1)^{th}$ interface, hence the optical path becomes $2(\sum_{j=1}^{j=i-1} d_j)/cos\theta$ which is less than the prior case$(2(\sum_{j=1}^{j=i} d_j)/cos\theta)$. Still as θ further increases, the optical path length increases in the manner illustrated above. This takes place till θ surpasses $\theta_{c_{ww_1}}$ or reaches θ_{max}. It is worth mentioning that these fluctuations are less profound if a model with less N is adopted. This is because less number of interfaces is included which is a rough inaccurate approximation of the real underwater medium.

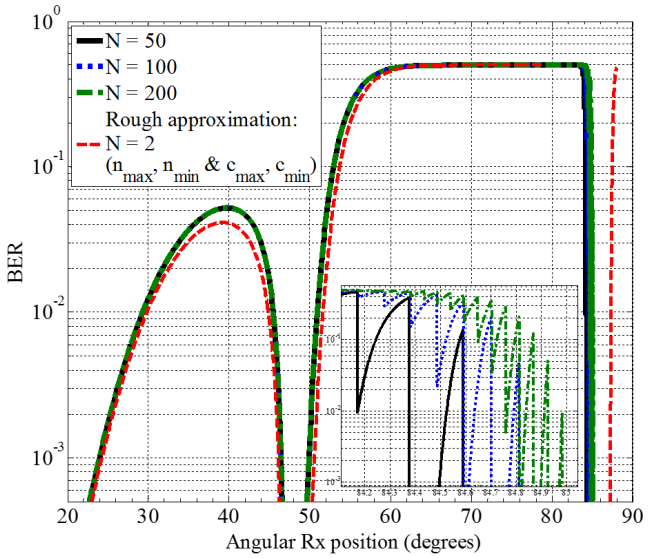

FIGURE 9. Two layer rough approximation in comparison to N layer model with different $N = 50$, 100 and 200 for a NLOS system with Tx rotation of 20°.

The interesting part about the above results is that there exists optimum Tx-Rx separations $(h_{Tx} + h_{Rx}).tan\theta$ for $\theta_{c,ww} \leq \theta \leq \theta_{max}$, where BER satisfies the FEC limit. According to Fig. 8(b), there may be four regions of possible communications at Tx orientation of 20°; at $0° < \theta < 24°, 48° < \theta < 50°, 84.35° < \theta < 84.5°$and $84.51° < \theta < 88°$. It is important herein to state that the last two regions of these mentioned above are highly sensitive to the number of layers N used to model the inhomogeneous underwater medium. A larger N ($\sim$200) is required for better approximation as appears in Fig. 9. Moreover, the rough approximation model previously mentioned in section $IV-C$ needs to be slightly altered to better model this specific case. The same rough approximation model of section $IV - C$ is applied, but with replacing c_{avg} with $c_{w_1} = \min(c(\lambda))$ and $c_{w_2} = \max(c(\lambda))$.

This shall be called the rotation rough approximation model. The rough approximation model of section $IV - C$ fails to model the BER performance at larger $\theta > \theta_{c,ww_i}$. Whereas the rotation rough approximation model gives an overestimation of the BER<FEC region at large$\theta > \theta_{c,ww_i}$ values. This dictates the importance of N layer modeling at this specific case at which the Tx is rotated such that $\theta > \theta_{c,ww_i}$.

E. NARROWING THE TRANSMITTED LIGHT CONE

Narrowing the emitted light cone from a Tx through light focusing results in illuminating a smaller annular area. Hence, per area, a higher light intensity is expected [5]. This may overcome optical path losses encountered by the travelling signal from Tx to the Rx. Fig. 10 shows the effect of narrowing the emitted light cone is studied in LOS and NLOS links in Fig.2.

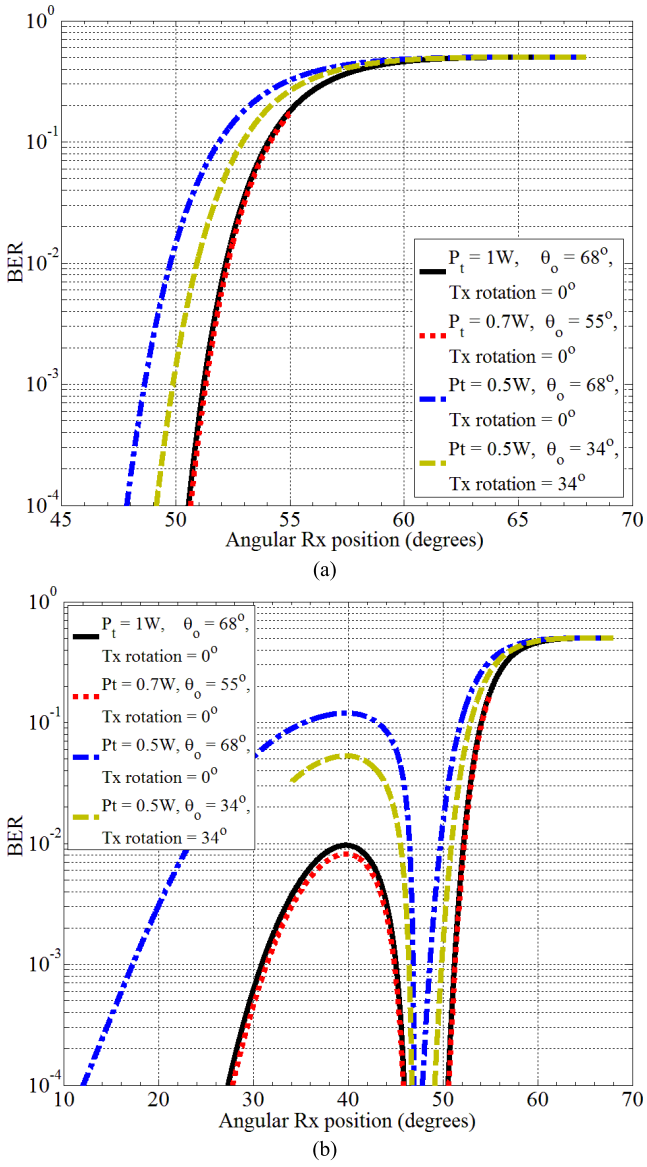

FIGURE 10. (a) Effect of narrowing LED divergence angle on BER for the LOS system in Fig. 2(a), $N = 50$. (b) Effect of narrowing LED divergence angle on BER for the NLOS system in Fig. 2(b), $N = 50$.

In Fig. 10(a), a Tx with P_t of 0.7W and θ_o of 55° gives a similar BER performance to a LOS system with a Tx with P_t equals to 1W and θ_o of 68°. This result proposes that energy efficient underwater communication is possible at no BER performance expense. By narrowing the Tx light cone by $\sim$ 19%, a possible decrease in the average transmitted power P_t by a 30% is obtained with the same BER performance. Moreover, a 34° rotated Tx with θ_o of 34° surpasses the BER performance of a system with unrotated (pointed upwards towards the sea-level) Tx with θ_o of 68° at the same P_t of 0.5W.

From Fig. 10(b), energy efficient underwater communication proves to be feasible such as in LOS case. An NLOS system with a Tx exhibiting a P_t of 0.7W and θ_o of 55°

has a similar BER performance equivalent to a Tx with P_t of 1W and θ_o of 68°. On the other hand, a 34° rotated Tx with θ_o of 34° with P_t of 0.5W offers a larger acceptable angular Rx position than an unrotated Tx with θ_o of 68° at the same P_t; i.e., $46° < \theta < 50°$ instead of $46° < \theta < 48°$. However, this comes at the expense of sacrificing the low BER region$0° < \theta < 17°$.

V. SUMMARY AND CONCLUSION

This work presents accurate models of LOS and NLOS vertical under water links utilizing VLC and their performances are evaluated and discussed. The inhomogeneity of the underwater environment is taken into consideration through modeling the propagation medium by stratified N layers. Each layer exhibits a refractive index and an extinction coefficient value adopted from the typical gradient profile of seawater. To the best of the authors' knowledge, expressing underwater inhomogeneity as stratified N layers has never been introduced in literature previously. Expressions of the received power are deduced with the aid of geometrical optics. Accurate link budget models for both LOS and NLOS links are introduced. Both the received power and BER are calculated for inhomogeneous underwater link for the sake of performance evaluation. Numerical examples are used to explain the proposed link budget models. The effect of modeling underwater inhomogeneous medium with different numbers of stratified layers N on the system performance is studied. Also, deviations from obtained results when considering a homogeneous underwater medium ($N = 1$) are illustrated and justified. In this work, modeling an inhomogeneous underwater environment with arbitrary values of N showed that $N = 1$ is not an accurate approximation to the real inhomogeneous underwater medium. It is true that the BER behaviour seems to be the same as for larger N. However, using $N = 1$ homogeneous approach does not offer an accurate estimation of angular Rx positions θ that satisfy BER below the FEC limit. The smallest number of layers N that is sufficient to model the underwater inhomogeneous profile in this work is found to be $N = 50$. Fifty or more layers result in accurate perfromance estimation of LOS and NLOS link scenarios in this work. The inaccuracy in angular Rx positions θ exhibiting BER $<$ FEC limit due to modeling underwater environment with a lower N may be overlooked for small depths. But it is more profound when larger depths are considered. This is due to the horizontal Tx- Rx separation expression, $(h_{Tx} + h_{Rx})tan\theta$, which exhibits a larger value at larger depths; i.e., larger $h_{Tx,Rx}$, for both LOS and NLOS links.

The deduced N layer model is also used to evaluate the effect of Tx orientation on the received power and BER for LOS and NLOS links. For LOS links with best performance, the Tx should be pointed upwards facing the sea-level. For NLOS links, BER<FEC may be obtained for large angular Rx positions θ when Tx is rotated with an angle exceeding critical angle values θ_{c,ww_i}.

Moreover, the possibility of a Tx power reduction of $30\% - 50\%$ in UWVLC links is found to be linked with Tx rotation and light cone focusing. Deduced mathematical expressions show that focusing the emitted light cone by 50% for the same P_t results in an increase of ∼3% in the angular Rx position (θ). On the other hand, link performance is proved to be the same when narrowing the emitted light cone by 19% and using a Tx with a 30% reduced power. Hence, energy efficient UWVLC links are proven to be possible through narrowing the Tx light cone.

A rough estimation of underwater link behaviour is also proposed by expressing the underwater environment as a simple bilayer model. The proposed bilayer model gives a very close estimation to results obtained using $N = 50 - 100$ layers. This allows for the estimation of the underwater link behaviour without tedious calculations. The optical parameters of these two layers are 1) n_{w_1} and n_{w_2} which are the maximum and minimum refractive indices given by (2), and 2) average extinction coefficient given by: $c_{avg} = [max\,(c\,(\lambda))+ \min(c(\lambda))]/2$.

The significance of this work follows from providing a means to accurate calculations of LOS and NLOS link budgets with consideration of underwater environment inhomogeneity. When underwater inhomogeneity is overlooked, the resulting received power is found to be overestimated than the actual one. Therefore, the value of this work is to present precise link budget calculation model to accurately estimate the transmitter coverage area to satisfy the required quality of service at the Rx's end in real life.

REFERENCES

[1] *James Cameron Now at Ocean's Deepest Point*. [Online]. Available: http://news.nationalgeographic.com/news/2012/03/120325-james-cameron-mariana-trench-challenger-deep-deepest-science-sub/

[2] Z. Zeng, S. Fu, H. Zhang, Y. Dong, and J. Cheng, "A survey of underwater optical wireless communications," *IEEE Commun. Surveys Tuts.*, vol. 19, no. 1, pp. 204–238, 1st Quart., 2017, doi: 10.1109/COMST.2016.2618841.

[3] Z. Zeng, "A survey of underwater wireless optical communication," M.S. thesis, Dept. Elect. Eng., Univ. British Columbia, Vancouver, BC, Canada, 2015.

[4] H. Kaushal and G. Kaddoum, "Underwater optical wireless communication," *IEEE Access*, vol. 4, pp. 1518–1547, 2016, doi: 10.1109/ACCESS.2016.2552538.

[5] C. Wang, H. Y. Yu, and Y. J. Zhu, "A long distance underwater visible light communication system with single photon avalanche diode," *IEEE Photon. J.*, vol. 8, no. 5, pp. 1–11, Oct. 2016, doi: 10.1109/JPHOT.2016.2602330.

[6] W. Cox and J. Muth, "Simulating channel losses in an underwater optical communication system," *J. Opt. Soc. Amer. A, Opt. Image Sci.*, vol. 31, no. 5, pp. 920–934, 2014.

[7] S. Watson *et al.*, "High speed visible light communication using blue GaN laser diodes," *Proc. SPIE*, vol. 9991, p. 99910A, Oct. 2016.

[8] M. V. Jamali *et al.*, "Statistical distribution of intensity fluctuations for underwater wireless optical channels in the presence of air bubbles," in *Proc. Iran Workshop Commun. Inf. Theory (IWCIT)*, Tehran, Iran, 2016, pp. 1–6, doi: 10.1109/IWCIT.2016.7491626.

[9] M. V. Jamali, F. Akhoundi, and J. A. Salehi, "Performance characterization of relay-assisted wireless optical CDMA networks in turbulent underwater channel," *IEEE Trans. Wireless Commun.*, vol. 15, no. 6, pp. 4104–4116, Jun. 2016, doi: 10.1109/TWC.2016.2533616S.

[10] S. Arnon and D. Kedar, "Non-line-of-sight underwater optical wireless communication network," *J. Opt. Soc. Amer. A, Opt. Image Sci.*, vol. 26, no. 3, pp. 530–539, 2009.

[11] Y. Song, Z. Tong, B. Cong, X. Yu, M. Kong, and A. Lin, "A combined radio and underwater wireless optical communication system based on buoys," *J. Phys., Conf. Ser.*, vol. 679, p. 012030, nos. 1–5, 2016.
[12] A. R. Darlis, W. A. Cahyadi, D. Darlis, and Y.-H. Chung, "Underwater visible light communication using maritime channel," in *Proc. Conf. Korea Inst. Signal Process. Syst. (KISPS)*, Dec. 2016, pp. 1–3.
[13] L. J. Johnson, R. J. Green, and M. S. Leeson, "Underwater optical wireless communications: Depth dependent variations in attenuation," *Appl. Opt.*, vol. 52, no. 33, pp. 7867–7873, 2013.
[14] L. J. Johnson, R. J. Green, and M. S. Leeson, "Hybrid underwater optical/acoustic link design," in *Proc. 16th Int. Conf. Transparent Opt. Netw. (ICTON)*, Graz, Austria, 2014, pp. 1–4, doi: 10.1109/ICTON.2014.6876491.
[15] L. J. Johnson, R. J. Green, and M. S. Leeson, "The impact of link orientation in underwater optical wireless communication systems," in *Proc. Oceans-St. John's*, St. John's, NL, Canada, 2014, pp. 1–8, doi: 10.1109/OCEANS.2014.7003030.
[16] R. C. Millard and G. Seaver, "An index of refraction algorithm for seawater over temperature, pressure, salinity, density, and wavelength," *Deep Sea Res. A, Oceanograp. Res. Papers*, vol. 37, no. 2, pp. 1909–1926, 1990.
[17] *How Does Pressure Change With Ocean Depth?* [Online]. Available: https://oceanservice.noaa.gov/facts/pressure.html
[18] Z. Ghassemlooy, W. Papoola, and S. Rajbhandari, *Optical Wireless Communications: System and Channel Modeling With MATLAB*. Boca Raton, FL, USA: CRC Press, 2013, ch. 3.
[19] L. D. Talley, "Salinity patterns in the ocean," *The Earth System: Physical and Chemical Dimensions of Global Environmental Change* (Encyclopedia of Global Environmental Change), vol. 1, M. C. MacCracken and J. S. Perry, Eds. Hoboken, NJ, USA: Wiley, 2002, pp. 629–640.
[20] J. C. Palais, *Fiber Optic Communications*, Englewood Cliffs, NJ, USA: Prentice-Hall, 2005.
[21] P. Yeh, *Optical Waves in Layered Media* (Wiley Series in Pure and Applied Optics). Hoboken, NJ, USA: Wiley, 2005.

NOHA ANOUS received the B.Sc. and M.Sc. degrees in electronics and communications engineering from Ain Shams University, Cairo, Egypt, in 2006 and 2011, respectively, where she is currently pursuing the Ph.D. degree with the Faculty of Engineering. She is currently a Research Associate with Texas A&M University at Qatar. Her research interests include optical plasmonic sensors, angle-tolerant filter design, and visible light communications.

MOHAMED ABDALLAH (M'06–SM'13) received the B.Sc. degree from Cairo University in 1996, and the M.Sc. and Ph.D. degrees from The University of Maryland, College Park, in 2001 and 2006, respectively. From 2006 to 2016, he held academic and research positions with Cairo University and Texas A&M University at Qatar. He is currently a founding Faculty Member with the rank of Assistant Professor with the Information and Computing Technology Division, Hamad Bin Khalifa University. He was a recipient of the Research Fellow Excellence Award at Texas A&M University at Qatar in 2016, the best paper award in the IEEE First Workshop on Smart Grid and Renewable Energy in 2015, and the Nortel Networks Industrial Fellowship for five consecutive years, from 1999 to 2003. He has acquired $7M in research funding and published over 100 journal and conference papers, four book chapters, and four U.S. patents (one issued and three pending). His professional activities include a technical program committee member of several major IEEE conferences, a Technical Program Chair of the 10th International Conference on cognitive radio oriented wireless networks, and an Associate Editor for the IEEE TRANSACTIONS ON COMMUNICATIONS.

MURAT UYSAL (S'98–M'02–SM'07) received the B.Sc. and M.Sc. degree in electronics and communication engineering from Istanbul Technical University, Istanbul, Turkey, in 1995 and 1998, respectively, and the Ph.D. degree in electrical engineering from Texas A&M University, College Station, Texas, in 2001. He is currently a Full Professor and a Chair of the Department of Electrical and Electronics Engineering, Özyeğin University, Istanbul, Turkey. He also serves as the Founding Director of the Center of Excellence in Optical Wireless Communicaion Technologies. Prior to joining Özyeğin University, he was a tenured Associate Professor with the University of Waterloo, Canada, where he still holds an Adjunct Faculty position. His research interests are in the broad areas of communication theory and signal processing with a particular emphasis on the physical layer aspects of wireless communication systems in radio and optical frequency bands.

Prof. Uysal was a recipient of the Marsland Faculty Fellowship in 2004, NSERC Discovery Accelerator Supplement Award in 2008, the University of Waterloo Engineering Research Excellence Award in 2010, Turkish Academy of Sciences Distinguished Young Scientist Award in 2011, and Özyeğin University Best Researcher Award in 2014 among others. He served as the Chair of the Communication Theory Symposium of the IEEE ICC 2007, a Chair of the Communications and Networking Symposium of the IEEE CCECE 2008, a Chair of the Communication and Information Theory Symposium of IWCMC 2011, a TPC Co-Chair of the IEEE WCNC 2014, and a General Chair of the IEEE IWOW 2015. He currently serves on the editorial board of the IEEE TRANSACTIONS ON WIRELESS COMMUNICATIONS. In the past, he was an Editor for the IEEE TRANSACTIONS ON COMMUNICATIONS, the IEEE TRANSACTIONS ON VEHICULAR TECHNOLOGY, the IEEE COMMUNICATIONS LETTERS, the Wiley *Wireless Communications and Mobile Computing* Journal, Wiley *Transactions on Emerging Telecommunications Technologies*, and a Guest Editor of the IEEE JSAC Special Issues on Optical Wireless Communication in 2009 and 2015. He was involved in the organization of several IEEE conferences at various levels. Over the years, he has served on the technical program committee of over 100 international conferences and workshops in the communications area.

KHALID QARAQE (M'97–SM'00) was born in Bethlehem. He received the B.S. degree (Hons.) in electrical engineering from the University of Technology, Bagdad, Iraq, in 1986, the M.S. degree in electrical engineering from the University of Jordan, Amman, Jordan, in 1989, and the Ph.D. degree in electrical engineering from Texas A&M University, College Station, TX, USA, in 1997. From 1989 to 2004, he has held a variety positions in many companies and has over 12 years of experience in the telecommunication industry. He has involved in numerous GSM, CDMA, and WCDMA projects and has experience in product development, design, deployments, testing, and integration. He joined the Department of Electrical and Computer Engineering, Texas A&M University at Qatar, Doha, Qatar, in 2004, where he is currently a Professor. He has been awarded 15 research projects consisting of over USD 9.0 M from local industries in Qatar and the Qatar National Research Foundation. He has authored 90 journal papers in top IEEE journals, and published and presented 194 papers at prestigious international conferences. He has 13 book chapters published, two books slated to appear in 2015, four patents, and presented five tutorials and talks. His research interests include communication theory and its application to design and performance, analysis of cellular systems and indoor communication systems, mobile networks, broadband wireless access, cooperative networks, cognitive radio, diversity techniques, and beyond 4G systems. He was a recipient of the Itochu Professorship Award from 2013 to 2015, the Best Researcher Award from QNRF 2013, the Best Paper Award from the IEEE First Workshop On Smart Grid And Renewable Energy in 2015, the Best Paper Award from the IEEE Globecom 2014, the Best Poster Award from IEEE Dyspan Conference in 2012, the TAMUQ Research Excellence Award in 2010, the Best Paper Award from ComNet 2010, the Best Paper Award from CROWNCOM 2009, and the Best Paper Award from ICSPC 2000 and 2007.